

## Article

# Vitamin D Alleviates Cadmium-Induced Inhibition of Chicken Bone Marrow Stromal Cells' Osteogenic Differentiation In Vitro

Xishuai Tong<sup>1,2,3,†</sup>, Ying Zhang<sup>4,†</sup>, Yutian Zhao<sup>1,2,3</sup>, Yawen Li<sup>1,2,3</sup>, Tan Li<sup>1,2,3</sup>, Hui Zou<sup>1,2,3</sup>, Yan Yuan<sup>1,2,3</sup>, Jianchun Bian<sup>1,2,3</sup>, Zongping Liu<sup>1,2,3,\*</sup> and Jianhong Gu<sup>1,2,3,\*</sup>

<sup>1</sup> Joint International Research Laboratory of Agriculture and Agri-Product Safety of the Ministry of Education of China, Institutes of Agricultural Science and Technology Development, College of Veterinary Medicine, Yangzhou University, Yangzhou 225009, China; xstong@yzu.edu.cn (X.T.); zouhui@yzu.edu.cn (H.Z.); yuanyan@yzu.edu.cn (Y.Y.); jcbian@yzu.edu.cn (J.B.)

<sup>2</sup> Jiangsu Co-Innovation Center for Prevention and Control of Important Animal Infectious Diseases and Zoonoses, Yangzhou 225009, China

<sup>3</sup> Jiangsu Key Laboratory of Zoonosis, Yangzhou 225009, China

<sup>4</sup> National Health Commission Key Laboratory of Parasitic Disease Control and Prevention, Jiangsu Provincial Key Laboratory on Parasite and Vector Control Technology, Jiangsu Institute of Parasitic Diseases, Wuxi 214064, China; zhangying0707@yeah.net

\* Correspondence: liuzongping@yzu.edu.cn (Z.L.); jhgu@yzu.edu.cn (J.G.)

† These authors contributed equally to this work.

**Simple Summary:** The most physiologically active form of vitamin D is  $1\alpha, 25$ -dehydroxyvitamin D<sub>3</sub> ( $1\alpha, 25$ -[OH]<sub>2</sub>D<sub>3</sub>), which participates in the bone metabolic homeostasis of animals. In addition to the bone matrix, bone also includes bone-related cells, such as bone marrow stromal cells (BMSCs), osteoblasts, osteoclasts, etc. BMSCs can differentiate into osteoblasts, which are regulated by the Runt-related transcription factor 2 (Runx2) and other factors. Furthermore, type I collagen (Col1) is synthesized by osteoblasts and combines with hydroxyapatite to form normal bone matrix.  $1\alpha, 25$ -[OH]<sub>2</sub>D<sub>3</sub> promotes the secretion of Col1 in animals and stimulates bone mineralization. In addition, environmental heavy metal has accumulated toxicity in the different organs and tissues of animals, including in bone. Cadmium (Cd) is an element of heavy metals in nature that has osteotoxicity, including the destruction of the bone matrix and damage of bone-related cells (such as BMSCs and osteoblasts), and even inducing the apoptosis of bone-related cells. In this study, despite Cd having a certain toxicity on BMSCs and osteogenic differentiation from chicken embryos, our assessment of Cd osteotoxicity via  $1\alpha, 25$ -[OH]<sub>2</sub>D<sub>3</sub> suggested this mitigating effect was, indeed, improved. These signs indicate that  $1\alpha, 25$ -[OH]<sub>2</sub>D<sub>3</sub> can alleviate Cd-induced osteogenic toxicity in White Leghorn chickens in vitro.

**Abstract:** Vitamin D is a lipid soluble vitamin that is mostly used to treat bone metabolism-related diseases. In this study, the effect of Cd toxicity in vitro on osteogenic differentiation derived from BMSCs and the alleviating effect of  $1\alpha, 25$ -[OH]<sub>2</sub>D<sub>3</sub> were investigated. Cell index in real time was monitored using a Real-time cell analyzer (RTCA) system. The activity of alkaline phosphatase (ALP), and the calcified nodules and the distribution of Runx2 protein were detected using ALP staining, alizarin red staining, and immunofluorescence, respectively. Furthermore, the mitochondrial membrane potential and the apoptotic rate of BMSCs, the mRNA levels of *RUNX2* and type I collagen alpha2 (*COL1A2*) genes, and the protein expression of Col1 and Runx2 were detected using flow cytometry, qRT-PCR and western blot, respectively. The proliferation of BMSCs and osteogenic differentiation were enhanced after treatment with different concentrations of  $1\alpha, 25$ -[OH]<sub>2</sub>D<sub>3</sub> compared with the control group. However, 5  $\mu$ mol/L Cd inhibited the proliferation of BMSCs. In addition, 10 nmol/L  $1\alpha, 25$ -[OH]<sub>2</sub>D<sub>3</sub> attenuated the toxicity and the apoptosis of BMSCs treated by Cd, and also promoted the osteogenic differentiation including the activity of ALP, and the protein expression of Col1 and Runx2.  $1\alpha, 25$ -[OH]<sub>2</sub>D<sub>3</sub> can alleviate cadmium-induced osteogenic toxicity in White Leghorn chickens in vitro.



**Citation:** Tong, X.; Zhang, Y.; Zhao, Y.; Li, Y.; Li, T.; Zou, H.; Yuan, Y.; Bian, J.; Liu, Z.; Gu, J. Vitamin D Alleviates Cadmium-Induced Inhibition of Chicken Bone Marrow Stromal Cells' Osteogenic Differentiation In Vitro. *Animals* **2023**, *13*, 2544. <https://doi.org/10.3390/ani13152544>

Academic Editor: Alireza Seidavi

Received: 16 June 2023

Revised: 18 July 2023

Accepted: 1 August 2023

Published: 7 August 2023



**Copyright:** © 2023 by the authors. Licensee MDPI, Basel, Switzerland. This article is an open access article distributed under the terms and conditions of the Creative Commons Attribution (CC BY) license (<https://creativecommons.org/licenses/by/4.0/>).

**Keywords:**  $1\alpha$ ; 25-(OH) $_2$ D $_3$ ; cadmium (Cd); bone marrow stromal cells (BMSCs); osteogenic differentiation; White Leghorn

## 1. Introduction

Vitamin D is a lipid soluble vitamin, and is mostly used to treat bone metabolism-related diseases in animals, such as Osteoporosis (OP), Osteomalacia (OM), Multiple Osteosclerosis (MS), and Rheumatoid Arthritis (RA) [1–4]. Previous studies have shown that dietary supplementation with vitamin D $_3$  and calcium (Ca) has been observed to decrease the severity and the incidence of Tibial Dyschondroplasia (TD) in young broilers [5–7]. 7-dehydrocholesterol (7-DHC) derived from the skin of animal is converted to pro-vitamin D $_3$  under ultraviolet (290–315 nm) irradiation [8]. Under the action of 25-hydroxylase in liver and 25-hydroxyvitamin D-1 alpha-hydroxylase (also known as Cyp27b1) in kidney, vitamin D $_3$  generates  $1\alpha$ , 25-dehydroxyvitamin D $_3$  ( $1\alpha$ , 25-[OH] $_2$ D $_3$ ), which is the most physiologically active form and is involved in the dynamic homeostasis of Ca ions (Ca $^{2+}$ ) in vivo [9]. Vitamin D stimulates the vitamin D receptor (VDR) to promote the absorption of Ca $^{2+}$ , normalizing the Ca $^{2+}$  level of blood [10]. Active vitamin D accelerates the accumulation of Ca $^{2+}$  into bones when serum Ca $^{2+}$  is sufficient [11,12]. Osteoblast maturation derived from bone marrow stromal cells (BMSCs) is regulated by various transcription factors, such as Runt-related transcription factor 2 (Runx2) and type I collagen (Col1) [13]. Runx2 is a pivotal regulatory factor during the differentiation of BMSCs into osteoblasts, which then activates the transcription of Col1 to achieve bone remodeling [14–16]. Thus, Runx2 and Col1 are the multifunctional regulatory factors that are essential for osteoblastic differentiation.

A previous study found that 24R, 25-(OH) $_2$ D $_3$  (a metabolite of vitamin D $_3$  prohormone 25-[OH]D $_3$ ) can inhibit the proliferation of human bone marrow stromal cells (hBMSCs), while increasing alkaline phosphatase (ALP) activity and bone calcification [17]. Likewise, 10 nmol/L  $1\alpha$ , 25-(OH) $_2$ D $_3$  promoting osteoblast differentiation from hBMSCs by increasing the activity and the mRNA level of ALP, osteocalcin (OCN) production and Col1 expression [18]. Another study has demonstrated that  $1\alpha$ , 25-(OH) $_2$ D $_3$  enhanced the osteogenic differentiation of human periodontal ligament stem cells (hPDLSCs) [19]. However, Han et al. [20] reported that  $1\alpha$ , 25-(OH) $_2$ D $_3$  inhibited osteogenic differentiation from BMSCs by activating Wnt/ $\beta$ -catenin signaling and decreasing the expression of bone morphogenetic protein-2 (BMP-2). A high-dose concentration (100 nmol/L) of  $1\alpha$ , 25-(OH) $_2$ D $_3$  inhibited osteoblastic mineralization by suppressing the nuclear factor- $\kappa$ B (NF- $\kappa$ B) activation and Smad activation in primary osteoblast precursors or MC3T3 pre-osteoblastic cells [21]. In addition,  $1\alpha$ , 25-(OH) $_2$ D $_3$  plays a protective effect against hydrogen peroxide (H $_2$ O $_2$ )-induced apoptosis of nucleus pulposus-derived mesenchymal stem cells (NPMSCs) including the apoptosis rate and apoptosis-related protein expression, such as B cell lymphoma-2 (Bcl-2), Bcl-2 associated X-protein (Bax), and cleaved caspase-3 [22]. Therefore, vitamin D and/or its derivatives plays a vital role in the differentiation of osteoblast and/or BMSCs.

Cadmium (Cd) is a natural element that accumulates in various organs of animals and has the characteristics of chemical toxicity, long half-life and refractory decomposition [23–25]. Cd accumulates in the animal body through the food chain, and especially for the kidneys and bone is more toxic [26,27]. Importantly, Cd has a direct toxic effect on the tissues or cells of bone, and also indirectly affects bone metabolism through the toxicity of liver and kidney, including interfering with Ca and vitamin D metabolism [23,24,28–30]. Cd inhibits osteoblast differentiation derived from BMSCs, promotes adipocyte differentiation to inhibit BMSCs activity and bone matrix mineralization, thereby impairing bone metabolism and bone remodeling [29]. Likewise, Cd promoted the cytotoxicity of MC3T3-E1 subclone 14 cells through exportin-1 accumulation, DNA damage, the induction of cleaved caspase-3 protein, and inhibition of osteoblast-related protein expression, such as Runx2 and Col1 [31].

In addition, Cd induced apoptosis of primary osteoblasts in rats by upregulating the Bax/Bcl-2 ratio, and suppressing this action performed by autophagy activator rapamycin, while potentiated by autophagy inhibitor chloroquine (CQ) or small interfering RNA against Beclin1, which is an autophagy regulatory initiator [32]. In this study, the aim was to evaluate the alleviated effect of  $1\alpha, 25\text{-(OH)}_2\text{D}_3$  on Cd-inhibited osteogenic differentiation and Cd-enhanced cell apoptosis of BMSCs.

## 2. Materials and Methods

### 2.1. SPF- Grade Eggs

SPF-grade White Leghorn eggs were purchased from Shandong Yijida Biotechnology Co., Ltd. (Jining, China). The eggs were incubated at 37 °C and 60% humidity in the egg incubator (Dezhou Dingfeng Machinery Equipment Co., Ltd.; Dezhou, China) until they were 18 days old. This study strictly followed the recommendations of the *Guidelines for the Care and Use of Laboratory Animals* issued by the National Research Council. At the end of the incubation on day 18, all chicken embryos were humanely euthanized, and femur and tibia were separated for further testing. The experimental protocols were approved by the Animal Care and Use Committee of Yangzhou University (Approval ID: SYXK [Su] 2016–0020; Yangzhou, China).

### 2.2. Reagents

Alpha-minimum essential medium ( $\alpha$ -MEM) and Dulbecco modified Eagle's medium (DMEM) were purchased from Gibco (Grand Island, New York, NY, USA). Fetal bovine serum (FBS) was purchased from Beijing EallBio Biomedical Technology Co., Ltd. (Beijing, China).  $\beta$ -Glycerophosphate, BCIP<sup>®</sup>/NBT substrate solution, cadmium acetate, and Trizol reagent were purchased from Sigma–Aldrich (St. Louis, MO, USA). ALP staining and alizarin red staining kit were purchased from Beijing Solarbio Science & Technology Co., Ltd. (Beijing, China). 0.25% trypsin solution and electrochemiluminescence (ECL) chemiluminescence kit were purchased from Suzhou New Cell & Molecular Biotech Co., Ltd. (Suzhou, China). JC-1 staining solution was purchased from ThermoFisher (Waltham, MA, USA). Hoechst 33258 staining, BCA protein assay kit, RIPA lysis buffer and actin-tracker red-Rhodamine (phalloidin) probe were purchased from Beyotime Biotech. Inc. (Shanghai, China). HiScript Q RT SuperMix for qPCR (+gDNA wiper) was purchased from Nanjing Vazyme Biotech Co., Ltd. (Nanjing, Jiangsu, China). Hieff<sup>®</sup> qPCR SYBR Green Master Mix was purchased from Yeasen Biotechnology (Shanghai) Co., Ltd. (Shanghai, China). 5 × SDS-PAGE Loading Buffer was purchased from Bio-Rad Laboratories, Inc. (Hercules, CA, USA). Polyclonal antibodies against Runx2, Col1, Bax and Bcl-2, and monoclonal antibody against cleaved caspase-3 were purchased from Beijing Bioss Biotechnology Co., Ltd. (Beijing, China). Polyclonal antibody against glyceraldehyde-3-phosphate dehydrogenase (GAPDH), horseradish peroxidase (HRP)-conjugated goat anti-mouse and HRP-conjugated goat anti-rabbit were purchased from Cell Signaling Technology, Inc. (Danvers, MA, USA).

### 2.3. Cell Culture and Treatment

The femur and tibia of 18-day-old chicken embryos were separated as previously reported [33]. The BMSCs were flushed using  $\alpha$ -MEM without FBS. Cells were filtered using 300 mesh filter screens, and then centrifuged at 1000 r/min for 5 min. Cells ( $3 \times 10^6$ /mL at density) were resuspended in  $\alpha$ -MEM supplement with 10% FBS at 5% CO<sub>2</sub> with 37 °C. The medium was replaced every 2 days. The second generation of BMSCs was renewed to induced medium for osteogenic differentiation. Cells were divided into four group that included: only cells as the control group (only cells), 10 nmol/L  $1\alpha, 25\text{-(OH)}_2\text{D}_3$  (pre-treated for 6 h) group, an only 5  $\mu\text{mol/L}$  Cd group, and 10 nmol/L  $1\alpha, 25\text{-(OH)}_2\text{D}_3$  + 5  $\mu\text{mol/L}$  Cd group.

#### 2.4. Real-Time Cell Analyzer (RTCA) Dynamic Monitoring of BMSCs

DMEM medium (without FBS) was added to each E-plate well as reference lines for normalization using an xCelligence system (RTCA software 2.1; Roche, Basel, Switzerland) consistent with the manufacturer's protocol as previously reported [34,35]. We placed the E-plate (a cell placement plate) in the 37 °C incubator for 30 min, and then cells (the density of cell at  $5 \times 10^3/200 \mu\text{L}$ ) were added to each well as previously described [34]. Next, the cells were treated with  $1\alpha,25\text{-(OH)}_2\text{D}_3$  in different concentrations (1, 10, and 100 nmol/L). The medium was replaced every 2 days. The normalized cell index (NCI) was calculated. Impedance was recorded every 15 min during the cell exponential proliferative phase [34].

#### 2.5. ALP Staining and Alizarin Red Staining

The second-generation of BMSCs from chickens were seeded into a 6-well plate (the density of cells was  $3 \times 10^5/\text{mL}$ ), and changed to osteogenic induction medium (containing 10% FBS, 10 nmol/L dexamethasone, 10 mmol/L sodium  $\beta$ -glycerophosphate, and 50  $\mu\text{g}/\text{mL}$  ascorbic acid) when they grew to about 75%. BMSCs was treated with induction medium for 7 days, and then the medium was discarded and washed with phosphate-buffered saline solution (PBS) 3–5 times. The cells were fixed in 4% paraformaldehyde solution for 30 min. Cell fluid was discarded, and then washed with PBS 3–5 times. BCIP<sup>®</sup>/NBT substrate solution was added to the cells for 30 min at room temperature (25 °C). The solution was discarded, and then washed with PBS twice. The picture was captured using a DMI 3000B inverted phase contrast microscope (Leica, Germany) for further observation.

In addition, the BMSCs were suspended in osteogenic induction medium for 21 days. The induction medium was discarded, and the cells were washed with PBS 3–5 times. The ethanol (at a percent of 90) was added with the cells for 30 min at room temperature (25 °C). The solution was discarded, and then washed with PBS 3–5 times. Alizarin red staining solution was added with the cells at room temperature (25 °C). The images were recorded using a DMI 3000B inverted phase contrast microscope (Leica, Germany).

#### 2.6. Flow Cytometry Assay

Cells were collected and washed with PBS 2 times. Next, the cells were resuspended in  $1 \times$  Binding Buffer, and centrifuged at 1000 r/min for 10 min. The supernatant solution was discarded. Cells were incubated with Annexin V-FITC probe for 10 min, and then propidium iodide (PI) was added for 5 min at room temperature (25 °C) in the dark. PBS was added into each tube for detection of cell apoptosis using a FACS LSRFortess Flow cytometry assay machine (BD Biosciences; San Jose, CA, USA).

In addition, cells were digested using the 0.25% trypsin solution with EDTA for 30 s. The cells were collected using the 15 mL centrifuge tubes for washing with PBS twice. Cells were incubated with  $\alpha$ -MEM (supplemented with 10% FBS). The supernatant solution was discarded. Then, the JC-1 staining solution, at a ratio of 1:1, was added for 20 min after the end of incubation. Finally, the cells were washed using the JC-1 staining solution twice for detection of cell mitochondrial membrane potential using a FACS LSRFortess Flow cytometry assay machine.

#### 2.7. qRT-PCR

Total RNA was extracted using a Trizol reagent as previously reported [36]. Pure RNA was used to reverse transcribe into cDNA using a HiScript Q RT SuperMix kit for qPCR (+gDNA wiper). Then, the primer sequences (Table 1) were synthesized for qRT-PCR by using a Hieff<sup>®</sup> qPCR SYBR Green Master Mix kit. The reaction methods were as follows: 95 °C for 30 s; 40 cycles of 95 °C for 5 s, 60 °C for 34 s; and 60 °C for 15 s. The mRNA expression of target genes was determined using the  $2^{-\Delta\Delta\text{Ct}}$  method. Accordingly, GAPDH was used as the housekeeping gene for normalization.

**Table 1.** The primer sequences of target genes for qRT-PCR.

Gene Name	Primer Sequence (5'–3')	Gene Number	Length (bp)
<i>RUNX2</i>	Forward: AACCCAAACTTGCCCAACCA Reverse: AGTACGGCCTCCAAACGGA	NM_204128.2	114
<i>COL1A2</i>	Forward: ATGGTCCTAGAGGTCTGCGT Reverse: AGCCTCTCCAGATGGACCTT	NM_001079714.2	109
<i>GAPDH</i>	Forward: GGGTGGTGCTAAGCGTGTTA Reverse: ACCCTCCACAATGCCAAAGT	NM_204305.2	180

### 2.8. Immunoblotting

Total protein was extracted using a lysis buffer as previously reported [33]. Equal amounts of denatured protein were divided into each tube. For immunoblotting, total proteins (30 µg) were separated using 12% or 10% sodium dodecyl sulfate-polyacrylamide gel electrophoresis (SDS-PAGE) gels. At the end of electrophoresis, the gels were transferred onto the polyvinylidene fluoride (PVDF) membranes with diameters of 0.22 µm (or 0.45 µm). At the end of protein transfer, the membranes were blocked with 5% free-fat milk buffer (the free-fat milk powder diluted into Tris-buffered saline solution with 0.1% Tween-20 [TBST]) for 1 h at room temperature (25 °C). Primary antibodies were used to dilute into different concentrations (Runx2, Col1, Bax, Bcl-2, cleaved caspase-3, and GAPDH at 1:1000), and then incubated at a low temperature (4 °C) for 12 h. All membranes were washed with TBST solution 5 times (5 min each time). Then, the membranes were incubated with HRP-conjugated IgG for 1 h at room temperature (25 °C). Finally, the membranes were scanned using a Tanon-5200 ECL chemiluminescent imaging system (Shanghai, China). Accordingly, the blot bands were quantitative analysis for statistical calculation.

### 2.9. Immunofluorescence

The cultural medium was discarded and washed with PBS twice. Cells were fixed in 4% paraformaldehyde solution for 30 min at room temperature (25 °C). The PBS was discarded and cells were mixed with 0.4% Triton X-100 solution for 10 min. The transmembrane solution was removed and combined with 5% BSA blocking buffer for 30 min at room temperature (25 °C). Cells were incubated with primary antibodies to Runx2 and IgG for 12 h, the latter serving as a negative control. We re-collected the primary antibodies and washed them with PBS 5 times. Then, the second immunofluorescence antibody was incubated for 2 h in the dark. Phalloidin staining was added into the cells for 10 min at room temperature (25 °C). Cells were washed with PBS 5 times and we added the Hoechst 33258 staining for 10 min at room temperature (25 °C). The images were recorded using a TCS SP8 STED high-resolution laser confocal microscope (Leica, Germany).

### 2.10. Statistical Analysis

All experimental data were analyzed using a method of one-way analysis of variance (ANOVA) by SPSS 25.0 (IBM SPSS; Armonk, New York, NY, USA). All data are presented as mean ± standard deviation (SD).  $p < 0.05$  and  $p < 0.01$  indicated significant and extremely significant difference, respectively. All the experiments were performed in triplicate.

## 3. Results

### 3.1. The Effects of $1\alpha, 25\text{-(OH)}_2\text{D}_3$ on Osteogenic Differentiation of BMSCs from Chickens

It has been previously reported that  $1\alpha, 25\text{-(OH)}_2\text{D}_3$  has multiple regulatory effects, including cell proliferation and cell differentiation [20]. To detect the effects of  $1\alpha, 25\text{-(OH)}_2\text{D}_3$  on the proliferation of BMSCs from chicken embryos in vitro, the cell index was monitored using a RTCA dynamic system. The data showed that the BMSCs enters the logarithmic growth phase after treatment with  $1\alpha, 25\text{-(OH)}_2\text{D}_3$  for 24 h. Then, the cell index was observed with supplementation with different concentrations of  $1\alpha, 25\text{-(OH)}_2\text{D}_3$  (1, 10, and 100 nmol/L); the cell index was normalized to analyze the difference, and the cell index in the 100 nmol/L  $1\alpha, 25\text{-(OH)}_2\text{D}_3$  group was lower than the other groups. However,

in terms of cell index, there was no difference between 1 and 10 nmol/L  $1\alpha, 25\text{-(OH)}_2\text{D}_3$  (Figure 1A). Next, the mRNA levels of *RUNX2* and *COL1A2* were measured by qRT-PCR after treatment with different concentrations of  $1\alpha, 25\text{-(OH)}_2\text{D}_3$ ; it was found that 10 nmol/L  $1\alpha, 25\text{-(OH)}_2\text{D}_3$ , more than 10 nmol/L, significantly increased their levels compared with 0 nmol/L  $1\alpha, 25\text{-(OH)}_2\text{D}_3$  (Figure 2B). Correspondingly, the expression of Col1 and Runx2 were enhanced after treatment with 1 and 10 nmol/L  $1\alpha, 25\text{-(OH)}_2\text{D}_3$  compared with 0 nmol/L  $1\alpha, 25\text{-(OH)}_2\text{D}_3$  (Figure 2C). These data indicated that  $1\alpha, 25\text{-(OH)}_2\text{D}_3$  promoted the osteogenic differentiation of BMSCs from chickens.

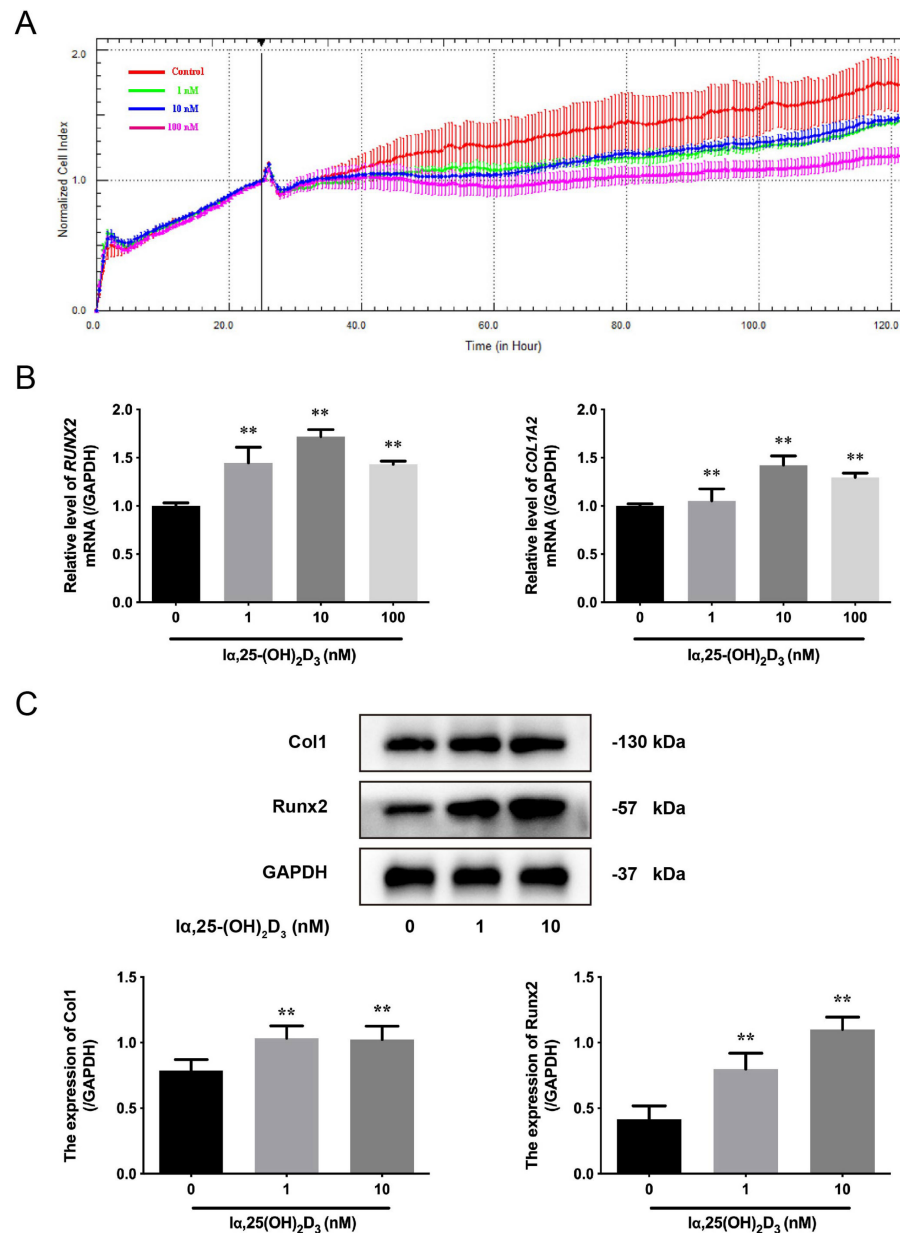


**Figure 1.** The effects of  $1\alpha, 25\text{-(OH)}_2\text{D}_3$  on osteogenic differentiation of BMSCs from chickens in vitro. (A) Cell index of BMSCs was monitored by the RTCA dynamic system after treatment with different concentrations (0, 1, 10, and 100 nmol/L) of  $1\alpha, 25\text{-(OH)}_2\text{D}_3$ . (B) The mRNA levels of *RUNX2* and *COL1A2* in BMSCs were measured by qRT-PCR after treatment with different concentrations (0, 1, 10, and 100 nmol/L) of  $1\alpha, 25\text{-(OH)}_2\text{D}_3$ . \*\*  $p < 0.01$  vs. 0 nmol/L  $1\alpha, 25\text{-(OH)}_2\text{D}_3$ . (C) The expression of Col1 and Runx2 in BMSCs were detected by Western blot after treatment with different concentrations (0, 1, and 10 nmol/L) of  $1\alpha, 25\text{-(OH)}_2\text{D}_3$ . GAPDH was used as an internal reference protein. \*\*  $p < 0.01$  vs. 0 nmol/L  $1\alpha, 25\text{-(OH)}_2\text{D}_3$ .

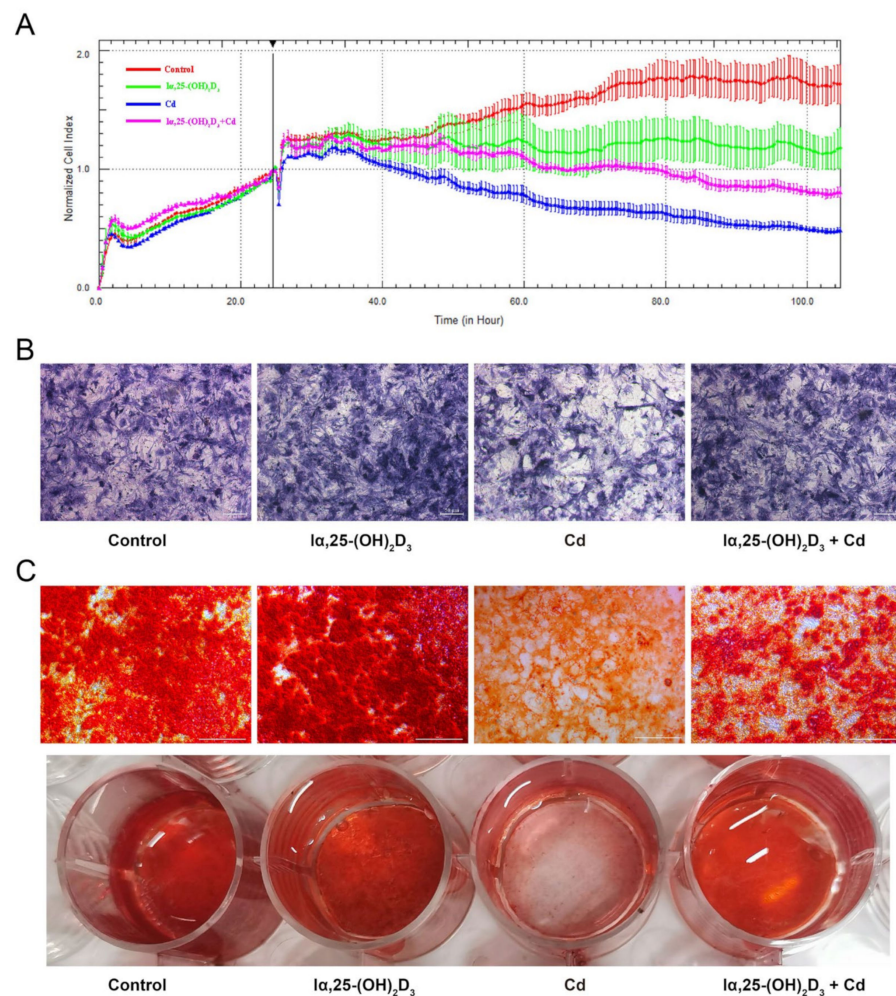


**Figure 2.** The effects of  $1\alpha, 25\text{-(OH)}_2\text{D}_3$  on Cd-inhibited osteogenic differentiation of BMSCs from chickens in vitro. (A) Cell index of BMSCs was monitored by the RTCA dynamic system after treatment with different groups. (B,C) The activity of ALP and the orange-red calcified nodules in BMSCs were observed using ALP staining and Alizarin red staining after treatment with different groups, respectively. (Control: only cells,  $1\alpha, 25\text{-(OH)}_2\text{D}_3$ : 10 nmol/L; Cd: 5  $\mu\text{mol/L}$  and  $1\alpha, 25\text{-(OH)}_2\text{D}_3$  + Cd: 10 nmol/L + 5  $\mu\text{mol/L}$ , respectively).

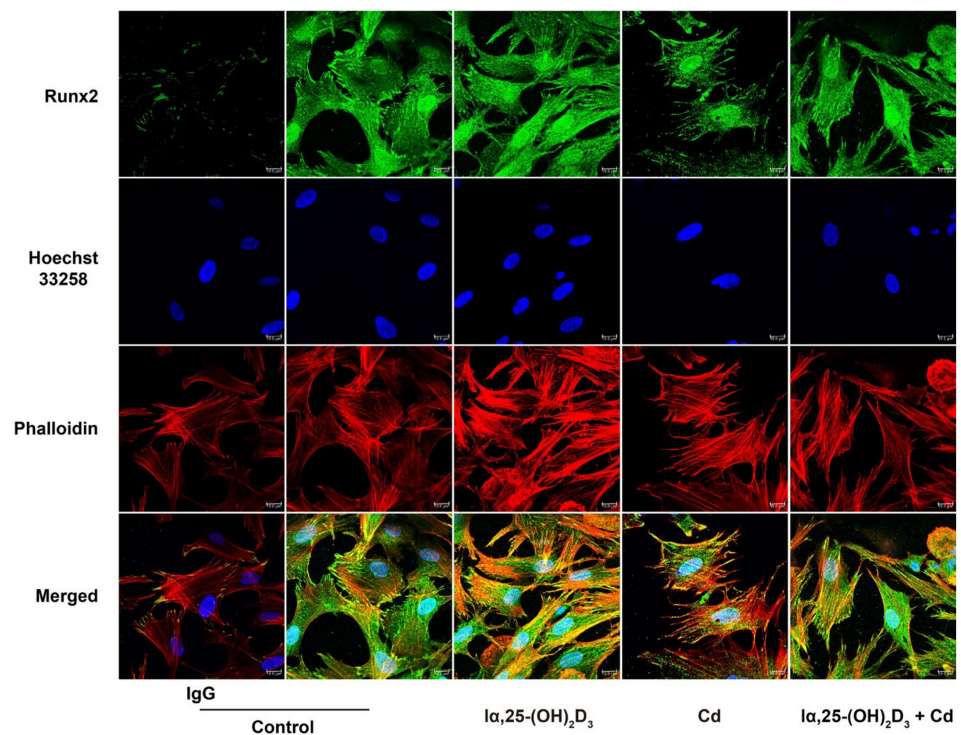
### 3.2. The Effects of $1\alpha, 25\text{-(OH)}_2\text{D}_3$ on Cd-Inhibited Osteogenic Differentiation of BMSCs from Chickens

To observe the proliferation of BMSCs treated by Cd, the cell proliferation, ALP staining and Alizarin red staining were utilized after different treatment in vitro. The results showed that 10  $\mu\text{mol/L}$  Cd has a more obviously inhibitory effect than the control group, but 10 nmol/L  $1\alpha, 25\text{-(OH)}_2\text{D}_3$  displayed an alleviated action on the Cd-inhibited proliferation of BMSCs from chickens (Figure 2A). As shown in Figure 2B, the activity of ALP in the 10 nmol/L  $1\alpha, 25\text{-(OH)}_2\text{D}_3$  group was enhanced compared with the control group, while the 5  $\mu\text{mol/L}$  Cd group decreased the purple black particles. However, the purple black particles in the 10 nmol/L  $1\alpha, 25\text{-(OH)}_2\text{D}_3$  co-treated with 5  $\mu\text{mol/L}$  Cd group were higher than the 5  $\mu\text{mol/L}$  Cd group. In addition, the color and stained area of orange-red calcified nodules in the 10 nmol/L  $1\alpha, 25\text{-(OH)}_2\text{D}_3$  group were enhanced using Alizarin red staining compared with the control group, while the 5  $\mu\text{mol/L}$  Cd group decreased the color and stained area of orange-red calcified nodules. Compared with the 5  $\mu\text{mol/L}$  Cd group, the color and stained area of orange-red calcified nodules in the the 10 nmol/L  $1\alpha, 25\text{-(OH)}_2\text{D}_3$  co-treated with the 5  $\mu\text{mol/L}$  Cd group were restored (Figure 2C). These data demonstrated the alleviating effects of  $1\alpha, 25\text{-(OH)}_2\text{D}_3$  on Cd-inhibited osteogenic differentiation of BMSCs from chickens.

### 3.3. The Distribution of Runx2 during $1\alpha, 25\text{-(OH)}_2\text{D}_3$ on Cd-Induced Osteogenic Differentiation of BMSCs from Chickens

As shown in Figure 3, the fluorescence intensity of Runx2 was enhanced after treatment with 10 nmol/L  $1\alpha, 25\text{-(OH)}_2\text{D}_3$  compared with the control group, and the IgG as a negative control. Furthermore, the 5  $\mu\text{mol/L}$  Cd group significantly attenuated the Runx2 fluorescence intensity compared with the control group. The Runx2 fluorescence intensity was augmented in the 10 nmol/L  $1\alpha, 25\text{-(OH)}_2\text{D}_3$  co-treated with 5  $\mu\text{mol/L}$  Cd group compared with the 5  $\mu\text{mol/L}$  Cd group (Figure 3A,B). These data showed that  $1\alpha, 25\text{-(OH)}_2\text{D}_3$  can alleviate the inhibitory effect of Runx2 in Cd-induced osteogenic differentiation of BMSCs from chickens.

A



B

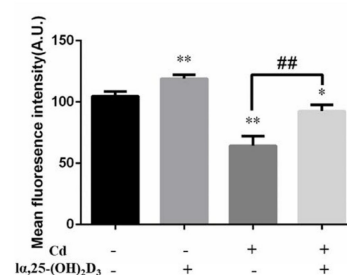


**Figure 3.** The distribution of Runx2 during  $1\alpha, 25\text{-(OH)}_2\text{D}_3$  on Cd-inhibited osteogenic differentiation of BMSCs from chickens in vitro. (A) Green fluorescence indicates the Runx2 distribution using a primary antibody, blue indicates the nucleus using the Hoechst 33258 dye, and red indicates the F-actin using a Phalloidin dye. (B) The mean fluorescence intensity of Runx2 was analyzed after treatment with different group. \*  $p < 0.05$ , \*\*  $p < 0.01$  vs. Control group; ##  $p < 0.01$  vs. Cd group. (Control: only cells,  $1\alpha, 25\text{-(OH)}_2\text{D}_3$ : 10 nmol/L; Cd: 5  $\mu\text{mol/L}$  and  $1\alpha, 25\text{-(OH)}_2\text{D}_3$  + Cd: 10 nmol/L + 5  $\mu\text{mol/L}$ , respectively).

### 3.4. The Effects of $\alpha, 25\text{-(OH)}_2\text{D}_3$ on Markers of Cd-Inhibited Osteogenic Differentiation of BMSCs from Chickens

To further verify the osteogenic differentiation of BMSCs from chickens, the expression of osteoblastic markers was examined after different treatments in vitro. The results showed that the mRNA levels of *RUNX2* and *COL1A2* in the  $\alpha, 25\text{-(OH)}_2\text{D}_3$  group were higher than the control group, but the 5  $\mu\text{mol/L}$  Cd group decreased their levels. Compared with the 5  $\mu\text{mol/L}$  Cd group, the levels of *RUNX2* and *COL1A2* mRNA in the 10 nmol/L  $\alpha, 25\text{-(OH)}_2\text{D}_3$  co-treated with 5  $\mu\text{mol/L}$  Cd group was augmented (Figure 4A). Correspondingly, the protein expression of Col1 and Runx2 showed the same trend with different treatments (Figure 4B). These results showed that  $\alpha, 25\text{-(OH)}_2\text{D}_3$  can attenuate the inhibitory effects on the expression of markers in Cd-inhibited osteogenic differentiation of BMSCs from chickens.

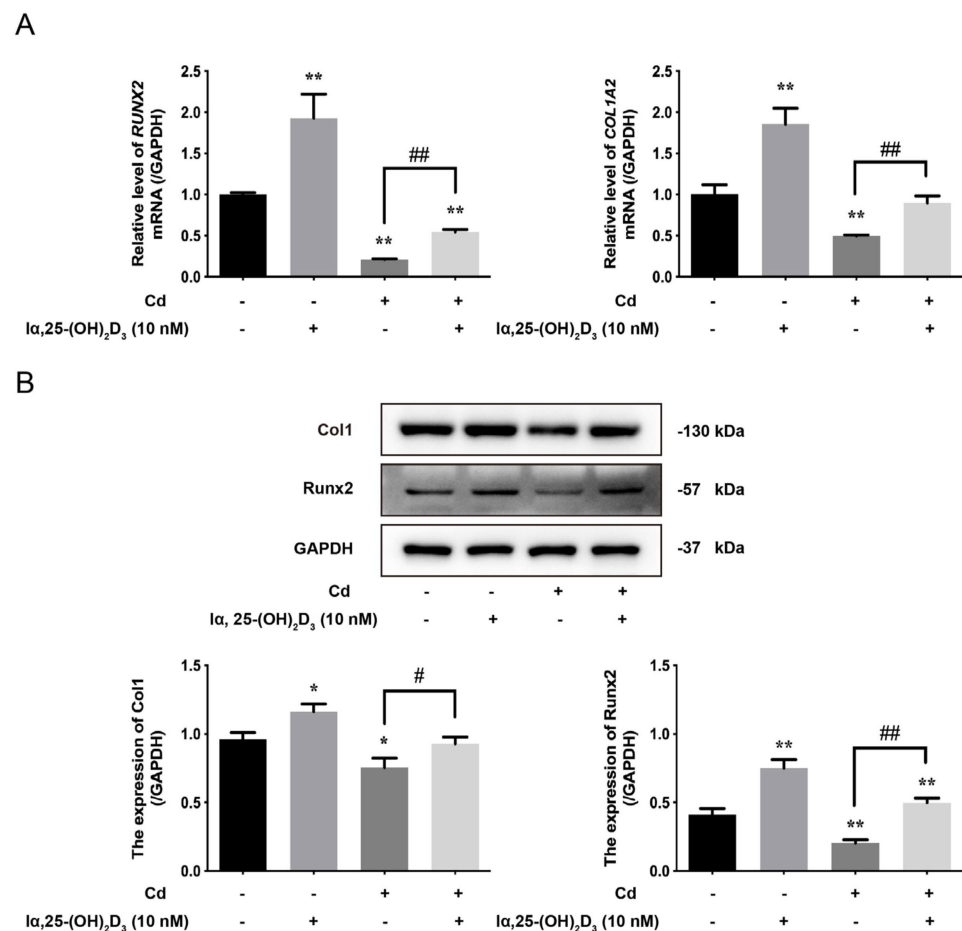


**Figure 4.** The effects of  $\alpha, 25\text{-(OH)}_2\text{D}_3$  on markers of Cd-inhibited osteogenic differentiation of BMSCs from chickens in vitro. (A) The mRNA levels of *RUNX2* and *COL1A2* in BMSCs were measured by qRT-PCR after treatment with different groups. \*\*  $p < 0.01$  vs. Control group; ##  $p < 0.01$  vs. Cd group. (B) The expression of Col1 and Runx2 in BMSCs were detected by Western blot after treatment with different groups. GAPDH was used as an internal reference protein. \*  $p < 0.05$ , \*\*  $p < 0.01$  vs. Control group; #  $p < 0.05$ , ##  $p < 0.01$  vs. Cd group. (Control: only cells,  $\alpha, 25\text{-(OH)}_2\text{D}_3$ : 10 nmol/L; Cd: 5  $\mu\text{mol/L}$  and  $\alpha, 25\text{-(OH)}_2\text{D}_3$  + Cd: 10 nmol/L + 5  $\mu\text{mol/L}$ , respectively).

### 3.5. The Effects of $\alpha, 25\text{-(OH)}_2\text{D}_3$ on Mitochondrial Membrane Potential and Apoptosis in Cd-Inhibited Osteogenic Differentiation of BMSCs from Chickens

Next, the mitochondrial membrane potential of BMSCs was detected after different treatments in vitro; the results showed that there was no significant difference between  $\alpha, 25\text{-(OH)}_2\text{D}_3$  group and the control group. However, 5  $\mu\text{mol/L}$  Cd decreased the mitochondrial membrane potential of BMSCs. Furthermore, the mitochondrial membrane

potential of BMSCs in the 10 nmol/L  $1\alpha, 25\text{-(OH)}_2\text{D}_3$  co-treated with 5  $\mu\text{mol/L}$  Cd group was higher than that in the 5  $\mu\text{mol/L}$  Cd group (Figure 5A). In addition, the apoptosis rate and apoptosis protein expression were measured after different treatments; the results showed that the apoptosis rate in the  $1\alpha, 25\text{-(OH)}_2\text{D}_3$  group had no change compared with the control group, but the apoptosis rate was increased in the 5  $\mu\text{mol/L}$  Cd group. The apoptosis rate in the 10 nmol/L  $1\alpha, 25\text{-(OH)}_2\text{D}_3$  co-treated with 5  $\mu\text{mol/L}$  Cd group was lower than the Cd group (Figure 5B). Correspondingly, the ratio of Bax/Bcl-2 was decreased in the  $1\alpha, 25\text{-(OH)}_2\text{D}_3$  group compared with the control group, but 5  $\mu\text{mol/L}$  Cd increased the ratio of Bax/Bcl-2. The ratio of Bax/Bcl-2 and the expression of cleaved caspase-3 in the 10 nmol/L  $1\alpha, 25\text{-(OH)}_2\text{D}_3$  co-treated with 5  $\mu\text{mol/L}$  Cd group were lower than the 5  $\mu\text{mol/L}$  Cd group (Figure 5C). These data demonstrated that  $1\alpha, 25\text{-(OH)}_2\text{D}_3$  can alleviate the apoptosis in Cd-inhibited osteogenic differentiation of BMSCs from chickens.

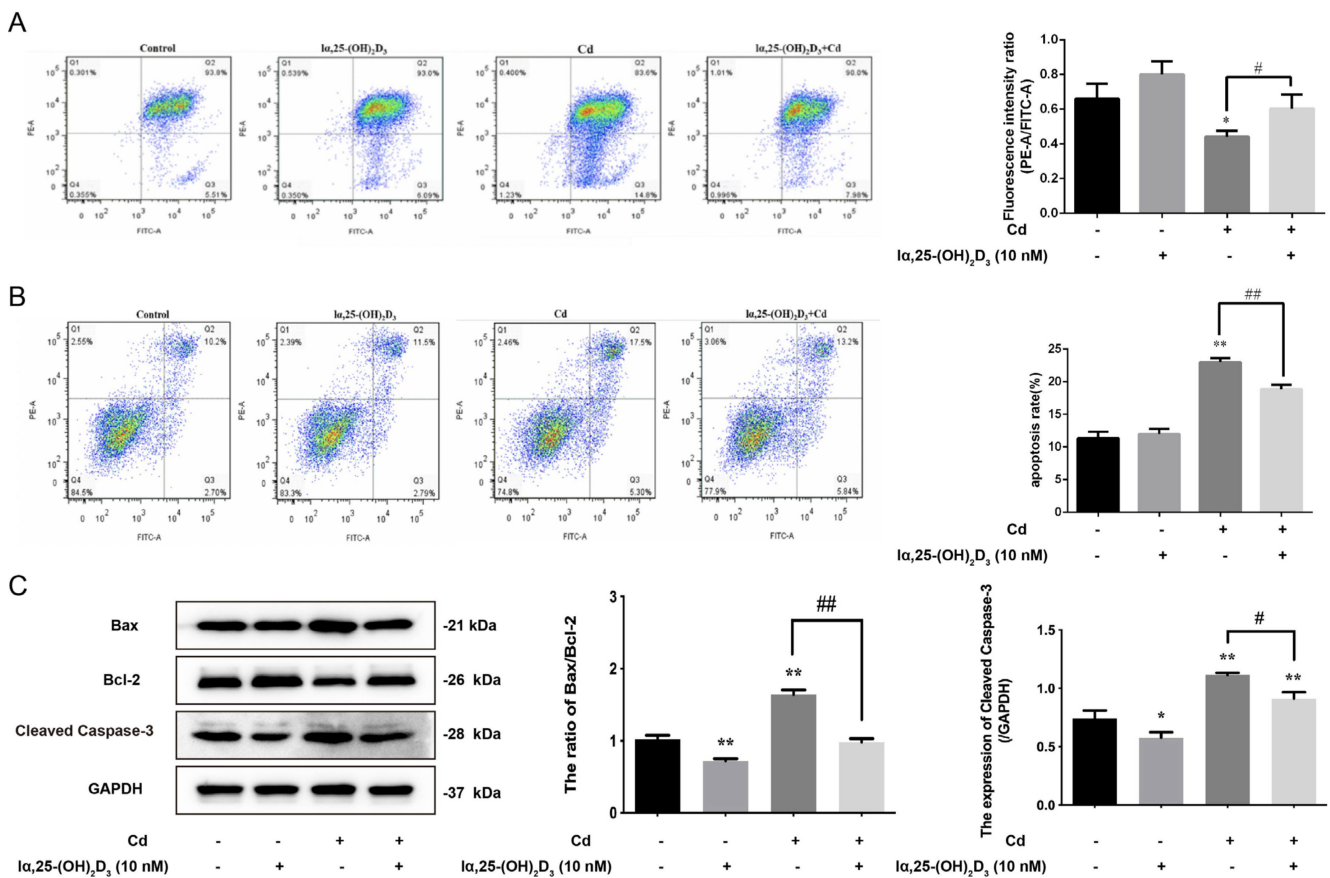


**Figure 5.** The effects of  $1\alpha, 25\text{-(OH)}_2\text{D}_3$  on mitochondrial membrane potential and apoptosis in Cd-inhibited osteogenic differentiation of BMSCs from chickens in vitro. (A,B) The mitochondrial membrane potential and apoptosis rate were measured by flow cytometry after treatment with different groups. ##  $p < 0.01$ , #  $p < 0.05$  vs. Cd group. (C) the ratio of Bax/Bcl-2 and the expression of cleaved caspase-3 were detected by Western blot after treatment with different groups. GAPDH was used as an internal reference protein. \*  $p < 0.05$ , \*\*  $p < 0.01$  vs. Control group; ##  $p < 0.01$  vs. Cd group. (Control: only cells,  $1\alpha, 25\text{-(OH)}_2\text{D}_3$ : 10 nmol/L; Cd: 5  $\mu\text{mol/L}$  and  $1\alpha, 25\text{-(OH)}_2\text{D}_3$  + Cd: 10 nmol/L + 5  $\mu\text{mol/L}$ , respectively).

#### 4. Discussion

Vitamin D<sub>3</sub> is mainly produced by ultraviolet rays in the human skin (around 80–90%), and is also sourced from daily diet (around 2000–4000 IU on average) [37]. Vitamin D is a critical regulator for bone metabolism and Ca<sup>2+</sup> balance by binding to its receptor VDR, and is involved in the differentiation and proliferation of cells, such as in the osteogenic differentiation of BMSCs [38,39]. Importantly,  $1\alpha, 25\text{-(OH)}_2\text{D}_3$ , the principally active form

of vitamin D, promoted the proliferation and migration of BMSCs in Sprague–Dawley (SD) rats [38].  $1\alpha, 25\text{-(OH)}_2\text{D}_3$  has an up-regulated effect in hBMSCs or MC3T3-E1 osteoblastic cells through increasing the mRNA levels of *RUNX2*, *COL1A1* (a component of type I collagen alpha 1), *OCN*, and *ALP* [40,41]. Runx2 and Col1 are key osteogenic potential markers during osteoblast differentiation of gingiva-derived mesenchymal stem cells (GMSCs) [42]. Runx2 as a major biomarker of osteoblast differentiation, is a widely used transcription factor for osteoblasts [43,44]. Likewise, Col1 is also known as an early osteogenic marker, and its early expression represents an early stage of maturation [42,45]. Col1 has a triple helix comprising two alpha 1 chains and one alpha 2 chain [46]. However, the mutation of *COL1A1* in induced pluripotent stem cells (iPSCs) from osteogenesis imperfecta (OI) may result in bone fragility and repeated fractures [40,47]. Correspondingly, the mutation of *COL1A2* can cause Osteogenesis Imperfecta (OI), and is close to the central region of the helical chain; the osteoblast differentiation ability is affected [48–50]. In this study, the proliferation of BMSCs from chickens was suppressed after treatment with different concentrations (1, 10, and 100 nmol/L) of  $1\alpha, 25\text{-(OH)}_2\text{D}_3$ . However, 10 nmol/L  $1\alpha, 25\text{-(OH)}_2\text{D}_3$  increased the mRNA levels of *RUNX2* and *COL1A2* and the protein expression of Runx2 and Col1 during osteogenic differentiation of BMSCs from chickens. These data are similar to those previously reported, while the species are different [40,41].

A previous study investigated that  $\text{CdCl}_2$  caused a reduction in cell activity in BMSCs from rats, nuclear breakage and chromatin condensation, and cytoplasm shrinkage [51]. A low concentration (0.1 or 0.2  $\mu\text{mol/L}$ ) of  $\text{CdCl}_2$  decreased the biomarker genes of bone marrow mesenchymal stem cells (BMMSCs) in SD rats, such as *ALP*, *RUNX2*, *OCN*, *osteopontin* (*OPN*), and *osterix* (*OSX*), as well as down-regulating the expression of *ALP* and *Runx2*, even *ALP* activity and the numbers of mineralization nodules, which were evaluated by *ALP* staining and Alizarin red staining, respectively [52]. Generally, the *ALP* staining was used to assess the *ALP* activity, which is also an early biomarker for osteogenic differentiation [52]. In addition, the mineralized nodules are usually observed at terminal differentiation, and are determined by Alizarin red staining as a late phase marker of osteogenic differentiation [53]. Consistent with *ALP* staining for decreasing the purple black particles, Cd reduced the orange-red mineralized nodules by Alizarin red staining. As Cd decreased the early and late marker of osteogenic differentiation, we further observed the distribution of Runx2 protein using immunofluorescence. It was found that Cd reduced the fluorescence intensity of Runx2 during the osteogenic differentiation of BMSCs from chickens. Correspondingly, Cd decreased the mRNA levels and the protein expression of osteogenic differentiation factors including Runx2 and Col1. Finally, the mitochondrial membrane potential of BMSCs from chickens was measured by flow cytometry; it was found that Cd reduced the mitochondrial membrane potential. As is well known, mitochondria dysfunction caused by a decrease in mitochondrial membrane potential is associated with cell apoptosis, including apoptosis rate, the abnormal expression of Bax/Bcl-2 ratio, and the activation of caspase-3 [54,55]. These induced mitochondria damages can lead to the apoptosis of BMSCs in osteogenic differentiation, which was consistent with studies on Cd toxicity in different species [32,56].

Next, we further explored the effects of  $1\alpha, 25\text{-(OH)}_2\text{D}_3$  on Cd-inhibited osteogenic differentiation of BMSCs from chickens. Several studies have shown that the repairing action of BMSCs in tissue injury is due to its localization in the bone marrow matrix, with the potential to differentiate and replace damaged cells and secrete cytokines to regulate cellular microenvironments [57,58]. For example, BMSCs repair the testicular injury of rats, and this may be highly related to mitochondrial apoptosis [57]. In addition,  $1\alpha, 25\text{-(OH)}_2\text{D}_3$  has a novel role in DNA repair in various tissues or in some disease processes, such as in breast cancer, and  $1\alpha, 25\text{-(OH)}_2\text{D}_3$  enhances the stabilization of the 53BP1 levels and the blockage of cathepsin L (a positive biomarker for triple-negative breast cancer) to treat or mitigate the tumorigenesis [59]. Our previous study demonstrated that  $1\alpha, 25\text{-(OH)}_2\text{D}_3$  palliated Cd-induced toxicity of chondrocytes in chicken embryo, are accompanied by the up-regulation of mitochondrial membrane potential and down-regulation of apoptosis

rate and Bax/Bcl-2 ratio [33]. In this study, our data have shown that the  $1\alpha, 25\text{-(OH)}_2\text{D}_3$  increased the activity of ALP and orange-red calcified mineralized nodules, the distribution of Runx2, the levels of Runx2 and Col1 and mitochondrial membrane potential during Cd-inhibited osteogenic differentiation of chicken's BMSCs, while decreasing the apoptosis rate, Bax/Bcl-2 ratio, and activation of caspase-3. Therefore, these findings may provide new insight for repairing Cd-inhibited osteogenic differentiation of BMSCs from chickens.

In conclusion, Cd has a toxicity role in BMSCs and/or osteogenic differentiation in chickens, and reduces osteogenic mineralization by promoting cell apoptosis in vitro. Moreover,  $1\alpha, 25\text{-(OH)}_2\text{D}_3$  facilitates the osteogenic differentiation and mineralization of BMSCs from chickens, and alleviates the Cd-induced toxicity of cells (Figure 6). However, the regulatory mechanisms by which  $1\alpha, 25\text{-(OH)}_2\text{D}_3$  mitigates Cd-stimulated toxicity need to be further investigated in detail.

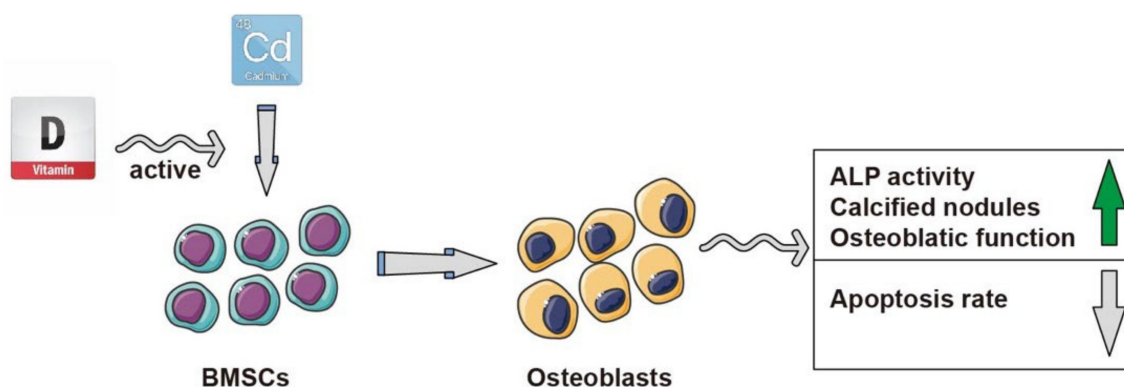


**Figure 6.** The schematic model of  $1\alpha, 25\text{-(OH)}_2\text{D}_3$ , which facilitates the osteogenic differentiation and mineralization from chicken's BMSCs, and alleviates Cd-induced toxicity of cells. Curved grey arrows represents mitigation effects, crooked arrows represent alleviating effects, and green straight arrow represents positive effects.

**Supplementary Materials:** The following supporting information can be downloaded at: <https://www.mdpi.com/article/10.3390/ani13152544/s1>, The origin western blot images of Col1, Runx2 and GAPDH in the Figure 1C; The origin western blot images of Col1, Runx2 and GAPDH in the Figure 4B; The origin western blot images of Bax, Bcl-2, Cleaved Caspase-3 and GAPDH in the Figure 5C.

**Author Contributions:** X.T., Y.Z. (Ying Zhang) and Y.Z. (Yutian Zhao) designed this project. X.T., Y.Z. (Yutian Zhao), Y.L. and T.L. performed the experiments and analyzed the results. X.T., Y.Z. (Ying Zhang) and J.G. drafted this manuscript. H.Z., Y.Y., J.B., Z.L. and J.G. revised the manuscript. All authors have read and agreed to the published version of the manuscript.

**Funding:** This research was supported by the National Natural Science Foundation of China (32102732, 31872534 and 31872533) and the Jiangsu Provincial Natural Science Foundation of China (BK20210806), and the project was funded by the Priority Academic Program Development of Jiangsu Higher Education Institutions (PAPD).

**Institutional Review Board Statement:** The animal experimental protocols were approved by the Animal Care and Use Committee of Yangzhou University (Approval ID: SYXK [Su] 2016-0020). (Approval date: 6 April 2016).

**Informed Consent Statement:** Not applicable.

**Data Availability Statement:** The raw data supporting the conclusions of this article will be made available by the authors. The origin western blot images presented in this study are available in Supplementary Materials.

**Acknowledgments:** We thank the Testing Center of Yangzhou University for providing technical support.

**Conflicts of Interest:** The authors declare that they have no conflict of interest.

## References

1. Martens, P.J.; Gysemans, C.; Verstuyf, A.; Mathieu, A.C. Vitamin D's Effect on Immune Function. *Nutrients* **2020**, *12*, 1248. [[CrossRef](#)] [[PubMed](#)]
2. Haussler, M.R.; Whitfield, G.K.; Kaneko, I.; Haussler, C.A.; Hsieh, D.; Hsieh, J.C.; Jurutka, P.W. Molecular mechanisms of vitamin D action. *Calcif. Tissue Int.* **2013**, *92*, 77–98. [[CrossRef](#)]
3. Chen, Y.H.; Yu, Z.; Fu, L.; Wang, H.; Chen, X.; Zhang, C.; Lv, Z.M.; Xu, D.X. Vitamin D<sub>3</sub> inhibits lipopolysaccharide-induced placental inflammation through reinforcing interaction between vitamin D receptor and nuclear factor kappa B p65 subunit. *Sci. Rep.* **2015**, *5*, 10871. [[CrossRef](#)] [[PubMed](#)]
4. Babazadeh, D.; Razavi, S.A.; Abd El-Ghany, W.A.; Cotter, P.F. Vitamin D Deficiency in Farm Animals: A Review. *Farm Anim. Health Nutr.* **2022**, *1*, 10–16. [[CrossRef](#)]
5. Warren, M.F.; Livingston, K.A. Implications of Vitamin D Research in Chickens can Advance Human Nutrition and Perspectives for the Future. *Curr. Dev. Nutr.* **2021**, *5*, nza018. [[CrossRef](#)] [[PubMed](#)]
6. Whitehead, C.C.; McCormack, H.A.; McTeir, L.; Fleming, R.H. High vitamin D<sub>3</sub> requirements in broilers for bone quality and prevention of tibial dyschondroplasia and interactions with dietary calcium, available phosphorus and vitamin A. *Br. Poult. Sci.* **2004**, *45*, 425–436. [[CrossRef](#)] [[PubMed](#)]
7. Fritts, C.A.; Waldroup, P.W. Effect of Source and Level of Vitamin D on Live Performance and Bone Development in Growing Broilers. *J. Appl. Poult. Res.* **2003**, *12*, 45–52. [[CrossRef](#)]
8. Battault, S.; Whiting, S.J.; Peltier, S.L.; Sadrin, S.; Gerber, G.; Maixent, J.M. Vitamin D metabolism, functions and needs: From science to health claims. *Eur. J. Nutr.* **2013**, *52*, 429–441. [[CrossRef](#)]
9. van Driel, M.; Koedam, M.; Buurman, C.J.; Hewison, M.; Chiba, H.; Uitterlinden, A.G.; Pols, H.A.; van Leeuwen, J.P. Evidence for auto/paracrine actions of vitamin D in bone: 1alpha-hydroxylase expression and activity in human bone cells. *FASEB J.* **2006**, *20*, 2417–2419. [[CrossRef](#)]
10. Holick, M.F. McCollum Award Lecture, 1994: Vitamin D—New horizons for the 21st century. *Am. J. Clin. Nutr.* **1994**, *60*, 619–630. [[CrossRef](#)]
11. Harahap, I.A.; Landrier, J.F.; Suliburska, J. Interrelationship between Vitamin D and Calcium in Obesity and Its Comorbid Conditions. *Nutrients* **2022**, *14*, 3187. [[CrossRef](#)] [[PubMed](#)]
12. Lips, P. Interaction between vitamin D and calcium. *Scand. J. Clin. Lab. Investig.* **2012**, *243*, 60–64.
13. Bianco, P.; Cao, X.; Frenette, P.S.; Mao, J.J.; Robey, P.G.; Simmons, P.J.; Wang, C.Y. The meaning, the sense and the significance: Translating the science of mesenchymal stem cells into medicine. *Nat. Med.* **2013**, *19*, 35–42. [[CrossRef](#)]
14. Komori, T. Roles of Runx2 in Skeletal Development. *Adv. Exp. Med. Biol.* **2017**, *962*, 83–93.
15. Javed, A.; Chen, H.; Ghori, F.Y. Genetic and transcriptional control of bone formation. *Oral Maxillofac. Surg. Clin. N. Am.* **2010**, *22*, 283–293. [[CrossRef](#)]
16. Cohen, M.M., Jr. Perspectives on RUNX genes: An update. *Am. J. Med. Genet. A* **2009**, *149A*, 2629–2646. [[CrossRef](#)]
17. Curtis, K.M.; Aenlle, K.K.; Roos, B.A.; Howard, G.A. 24R,25-dihydroxyvitamin D<sub>3</sub> promotes the osteoblastic differentiation of human mesenchymal stem cells. *Mol. Endocrinol.* **2014**, *28*, 644–658. [[CrossRef](#)] [[PubMed](#)]
18. Fromigué, O.; Marie, P.J.; Lomri, A. Differential effects of transforming growth factor beta2, dexamethasone and 1,25-dihydroxyvitamin D on human bone marrow stromal cells. *Cytokine* **1997**, *9*, 613–623. [[CrossRef](#)] [[PubMed](#)]
19. Ji, Y.; Zhang, P.; Xing, Y.; Jia, L.; Zhang, Y.; Jia, T.; Wu, X.; Zhao, B.; Xu, X. Effect of 1 $\alpha$ , 25-dihydroxyvitamin D<sub>3</sub> on the osteogenic differentiation of human periodontal ligament stem cells and the underlying regulatory mechanism. *Int. J. Mol. Med.* **2019**, *43*, 167–176. [[CrossRef](#)]
20. Han, X.; Zhu, N.; Wang, Y.; Cheng, G. 1,25(OH)<sub>2</sub>D<sub>3</sub> inhibits osteogenic differentiation through activating  $\beta$ -catenin signaling via downregulating bone morphogenetic protein 2. *Mol. Med. Rep.* **2020**, *22*, 5023–5032. [[CrossRef](#)]
21. Yamaguchi, M.; Weitzmann, M.N. High dose 1,25(OH)<sub>2</sub>D<sub>3</sub> inhibits osteoblast mineralization in vitro. *Int. J. Mol. Med.* **2012**, *29*, 934–938. [[PubMed](#)]
22. Wang, J.W.; Zhu, L.; Shi, P.Z.; Wang, P.C.; Dai, Y.; Wang, Y.X.; Lu, X.H.; Cheng, X.F.; Feng, X.M.; Zhang, L. 1,25(OH)<sub>2</sub>D<sub>3</sub> Mitigates Oxidative Stress-Induced Damage to Nucleus Pulposus-Derived Mesenchymal Stem Cells through PI3K/Akt Pathway. *Oxid. Med. Cell. Longev.* **2022**, *2022*, 1427110. [[CrossRef](#)]
23. Ma, Y.; Ran, D.; Zhao, H.; Song, R.; Zou, H.; Gu, J.; Yuan, Y.; Bian, J.; Zhu, J.; Liu, Z. Cadmium exposure triggers osteoporosis in duck via P2X7/PI3K/AKT-mediated osteoblast and osteoclast differentiation. *Sci. Total Environ.* **2021**, *750*, 141638. [[CrossRef](#)] [[PubMed](#)]
24. Genchi, G.; Sinicropi, M.S.; Lauria, G.; Carocci, A.; Catalano, A. The Effects of Cadmium Toxicity. *Int. J. Environ. Res. Public Health* **2020**, *17*, 3782. [[CrossRef](#)] [[PubMed](#)]
25. Kumar, S.; Sharma, A. Cadmium toxicity: Effects on human reproduction and fertility. *Rev. Environ. Health* **2019**, *34*, 327–338. [[CrossRef](#)]
26. McGrath, S.P. Keeping toxic cadmium out of the food chain. *Nat. Food* **2022**, *3*, 569–570. [[CrossRef](#)]
27. Chunhabundit, R. Cadmium Exposure and Potential Health Risk from Foods in Contaminated Area, Thailand. *Toxicol. Res.* **2016**, *32*, 65–72. [[CrossRef](#)]
28. Zhao, M.; Zhu, X.; Shan, D.; Huang, X.; Xu, Q. Metabolomics in liver injury induced by dietary cadmium exposure and protective effect of calcium supplementation. *Anal. Biochem.* **2022**, *641*, 114556. [[CrossRef](#)]

29. Rodríguez, J.; Mandalunis, P.M. Effect of cadmium on bone tissue in growing animals. *Exp. Toxicol. Pathol.* **2016**, *68*, 391–397. [[CrossRef](#)]
30. Ohta, H.; Ichikawa, M.; Seki, Y. Effects of cadmium intake on bone metabolism of mothers during pregnancy and lactation. *Tohoku J. Exp. Med.* **2002**, *196*, 33–42. [[CrossRef](#)]
31. Ou, L.; Wang, H.; Wu, Z.; Wang, P.; Yang, L.; Li, X.; Sun, K.; Zhu, X.; Zhang, R. Effects of cadmium on osteoblast cell line: Exportin 1 accumulation, p-JNK activation, DNA damage and cell apoptosis. *Ecotoxicol. Environ. Saf.* **2021**, *208*, 111668. [[CrossRef](#)]
32. Liu, W.; Dai, N.; Wang, Y.; Xu, C.; Zhao, H.; Xia, P.; Gu, J.; Liu, X.; Bian, J.; Yuan, Y.; et al. Role of autophagy in cadmium-induced apoptosis of primary rat osteoblasts. *Sci. Rep.* **2016**, *6*, 20404. [[CrossRef](#)] [[PubMed](#)]
33. Gu, J.; Li, S.; Wang, G.; Zhang, X.; Yuan, Y.; Liu, X.; Bian, J.; Tong, X.; Liu, Z. Cadmium Toxicity on Chondrocytes and the Palliative Effects of  $1\alpha, 25$ -Dihydroxy Vitamin D<sub>3</sub> in White Leghorns Chicken's Embryo. *Front. Vet. Sci.* **2021**, *8*, 637369. [[CrossRef](#)] [[PubMed](#)]
34. Tong, X.; Gu, J.; Song, R.; Wang, D.; Sun, Z.; Sui, C.; Zhang, C.; Liu, X.; Bian, J.; Liu, Z. Osteoprotegerin inhibit osteoclast differentiation and bone resorption by enhancing autophagy via AMPK/mTOR/p70S6K signaling pathway in vitro. *J. Cell. Biochem.* **2019**, *120*, 1630–1642. [[CrossRef](#)]
35. Zhao, H.; Liu, X.; Zou, H.; Dai, N.; Yao, L.; Zhang, X.; Gao, Q.; Liu, W.; Gu, J.; Yuan, Y.; et al. Osteoprotegerin disrupts peripheral adhesive structures of osteoclasts by modulating Pyk2 and Src activities. *Cell Adhes. Migr.* **2016**, *10*, 299–309. [[CrossRef](#)]
36. Tong, X.; Yu, G.; Liu, Q.; Zhang, X.; Bian, J.; Liu, Z.; Gu, J. Puerarin alleviates cadmium-induced oxidative damage to bone by reducing autophagy in rats. *Environ. Toxicol.* **2022**, *37*, 720–729. [[CrossRef](#)]
37. Pierrot-Deseilligny, C.; Souberbielle, J.C. Vitamin D and multiple sclerosis: An update. *Mult. Scler. Relat. Disord.* **2017**, *14*, 35–45. [[CrossRef](#)]
38. Jiang, X.; Huang, B.; Yang, H.; Li, G.; Zhang, C.; Yang, G.; Lin, F.; Lin, G. TGF- $\beta$ 1 is Involved in Vitamin D-Induced Chondrogenic Differentiation of Bone Marrow-Derived Mesenchymal Stem Cells by Regulating the ERK/JNK Pathway. *Cell. Physiol. Biochem.* **2017**, *42*, 2230–2241. [[CrossRef](#)]
39. Piek, E.; Sleumer, L.S.; van Someren, E.P.; Heuver, L.; de Haan, J.R.; de Grijis, I.; Gilissen, C.; Hendriks, J.M.; van Ravestein-van Os, R.I.; Bauerschmidt, S.; et al. Osteo-transcriptomics of human mesenchymal stem cells: Accelerated gene expression and osteoblast differentiation induced by vitamin D reveals c-MYC as an enhancer of BMP2-induced osteogenesis. *Bone* **2010**, *46*, 613–627. [[CrossRef](#)] [[PubMed](#)]
40. Lee, H.J.; Song, Y.M.; Baek, S.; Park, Y.H.; Park, J.B. Vitamin D Enhanced the Osteogenic Differentiation of Cell Spheroids Composed of Bone Marrow Stem Cells. *Medicina* **2021**, *57*, 1271. [[CrossRef](#)]
41. Kim, H.S.; Zheng, M.; Kim, D.K.; Lee, W.P.; Yu, S.J.; Kim, B.O. Effects of 1,25-dihydroxyvitamin D<sub>3</sub> on the differentiation of MC3T3-E1 osteoblast-like cells. *J. Periodontal Implant Sci.* **2018**, *48*, 34–46. [[CrossRef](#)] [[PubMed](#)]
42. Alnhash, A.Z.; Song, Y.-M.; Min, S.-K.; Lee, H.-J.; Kim, M.-J.; Park, Y.-H.; Park, J.-U.; Park, J.-B. Effects of Connective Tissue Growth Factor on the Cell Viability, Proliferation, Osteogenic Capacity and mRNA Expression of Stem Cell Spheroids. *Appl. Sci.* **2021**, *11*, 6572. [[CrossRef](#)]
43. Min, S.K.; Kim, M.; Park, J.B. Insulin-like growth factor 2-enhanced osteogenic differentiation of stem cell spheroids by regulation of Runx2 and Col1 expression. *Exp. Ther. Med.* **2021**, *21*, 383. [[CrossRef](#)] [[PubMed](#)]
44. Lv, H.; Yang, H.; Wang, Y. Effects of miR-103 by negatively regulating SATB2 on proliferation and osteogenic differentiation of human bone marrow mesenchymal stem cells. *PLoS ONE* **2020**, *15*, e0232695. [[CrossRef](#)]
45. Payr, S.; Rosado-Balmayor, E.; Tiefenboeck, T.; Schuseil, T.; Unger, M.; Seeliger, C.; van Griensven, M. Direct comparison of 3D and 2D cultivation reveals higher osteogenic capacity of elderly osteoblasts in 3D. *J. Orthop. Surg. Res.* **2021**, *16*, 13. [[CrossRef](#)]
46. Besio, R.; Chow, C.-W.; Tonelli, F.; Marini, J.C.; Forlino, A. Bone biology: Insights from osteogenesis imperfecta and related rare fragility syndromes. *FEBS J.* **2019**, *286*, 3033–3056. [[CrossRef](#)]
47. Jung, H.; Rim, Y.A.; Park, N.; Nam, Y.; Ju, J.H. Restoration of Osteogenesis by CRISPR/Cas9 Genome Editing of the Mutated COL1A1 Gene in Osteogenesis Imperfecta. *J. Clin. Med.* **2021**, *10*, 3141. [[CrossRef](#)]
48. Augusciak-Duma, A.; Witecka, J.; Sieron, A.L.; Janeczko, M.; Pietrzyk, J.J.; Ochman, K.; Galicka, A.; Borszewska-Kornacka, M.K.; Pilch, J.; Jakubowska-Pietkiewicz, E. Mutations in the COL1A1 and COL1A2 genes associated with osteogenesis imperfecta (OI) types I or III. *Acta Biochim. Pol.* **2018**, *65*, 79–86. [[CrossRef](#)]
49. Forlino, A.; Marini, J.C. Osteogenesis imperfecta. *Lancet* **2016**, *387*, 1657–1671. [[CrossRef](#)]
50. Li, H.; Jiang, X.; Delaney, J.; Franceschetti, T.; Bilic-Curcic, I.; Kalinovsky, J.; Lorenzo, J.A.; Grcevic, D.; Rowe, D.W.; Kalajzic, I. Immature osteoblast lineage cells increase osteoclastogenesis in osteogenesis imperfecta murine. *Am. J. Pathol.* **2010**, *176*, 2405–2413. [[CrossRef](#)]
51. Haussler, M.R.; Haussler, C.A.; Whitfield, G.K.; Hsieh, J.C.; Thompson, P.D.; Barthel, T.K.; Bartik, L.; Egan, J.B.; Wu, Y.; Kubicek, J.L.; et al. The nuclear vitamin D receptor controls the expression of genes encoding factors which feed the “Fountain of Youth” to mediate healthful aging. *J. Steroid Biochem. Mol. Biol.* **2010**, *121*, 88–97. [[CrossRef](#)] [[PubMed](#)]
52. Wu, L.; Wei, Q.; Lv, Y.; Xue, J.; Zhang, B.; Sun, Q.; Xiao, T.; Huang, R.; Wang, P.; Dai, X.; et al. Wnt/ $\beta$ -Catenin Pathway Is Involved in Cadmium-Induced Inhibition of Osteoblast Differentiation of Bone Marrow Mesenchymal Stem Cells. *Int. J. Mol. Sci.* **2019**, *20*, 1519. [[CrossRef](#)] [[PubMed](#)]
53. Yun, H.M.; Park, K.R.; Quang, T.H.; Oh, H.; Hong, J.T.; Kim, Y.C.; Kim, E.C. 2,4,5-Trimethoxydalbergiquinol promotes osteoblastic differentiation and mineralization via the BMP and Wnt/ $\beta$ -catenin pathway. *Cell Death Dis.* **2015**, *6*, e1819. [[CrossRef](#)] [[PubMed](#)]

54. Cao, X.; Fu, M.; Bi, R.; Zheng, X.; Fu, B.; Tian, S.; Liu, C.; Li, Q.; Liu, J. Cadmium induced BEAS-2B cells apoptosis and mitochondria damage via MAPK signaling pathway. *Chemosphere* **2021**, *263*, 128346. [[CrossRef](#)]
55. Abate, M.; Festa, A.; Falco, M.; Lombardi, A.; Luce, A.; Grimaldi, A.; Zappavigna, S.; Sperlongano, P.; Irace, C.; Caraglia, M.; et al. Mitochondria as playmakers of apoptosis, autophagy and senescence. *Semin. Cell Dev. Biol.* **2020**, *98*, 139–153. [[CrossRef](#)]
56. Li, S.; Baiyun, R.; Lv, Z.; Li, J.; Han, D.; Zhao, W.; Yu, L.; Deng, N.; Liu, Z.; Zhang, Z. Exploring the kidney hazard of exposure to mercuric chloride in mice: Disorder of mitochondrial dynamics induces oxidative stress and results in apoptosis. *Chemosphere* **2019**, *234*, 822–829. [[CrossRef](#)]
57. Wang, Y.-J.; Yan, J.; Zou, X.-L.; Guo, K.-J.; Zhao, Y.; Meng, C.-Y.; Yin, F.; Guo, L. Bone marrow mesenchymal stem cells repair cadmium-induced rat testis injury by inhibiting mitochondrial apoptosis. *Chem. Biol. Interact.* **2017**, *271*, 39–47. [[CrossRef](#)]
58. Yin, F.; Meng, C.; Lu, R.; Li, L.; Zhang, Y.; Chen, H.; Qin, Y.; Guo, L. Bone marrow mesenchymal stem cells repair spinal cord ischemia/reperfusion injury by promoting axonal growth and anti-autophagy. *Neural Regen. Res.* **2014**, *9*, 1665–1671.
59. Gonzalo, S. Novel roles of  $1\alpha,25(\text{OH})_2\text{D}_3$  on DNA repair provide new strategies for breast cancer treatment. *J. Steroid Biochem. Mol. Biol.* **2014**, *144 Pt A*, 59–64. [[CrossRef](#)]

**Disclaimer/Publisher’s Note:** The statements, opinions and data contained in all publications are solely those of the individual author(s) and contributor(s) and not of MDPI and/or the editor(s). MDPI and/or the editor(s) disclaim responsibility for any injury to people or property resulting from any ideas, methods, instructions or products referred to in the content.